

From concentric eyewall to annular hurricane: A numerical study with the cloud-resolved WRF model

Xiaqiong Zhou¹ and Bin Wang¹

Received 30 November 2008; accepted 7 January 2009; published 4 February 2009.

[1] Observations show that concentric eyewalls may lead to the formation of an annular hurricane (AH), but available radar and satellite images provide very limited information. By using the cloud-resolved Weather Research and Forecasting (WRF) model, the transformation from a non-AH to an AH through a concentric eyewall replacement cycle is simulated under a resting environment. The simulated hurricane experiences three distinct stages: the formation of a secondary eyewall, the eyewall replacement and the formation of an AH. The simulated eyewall succession and accompanying intensity change are qualitatively consistent with observations. The bottom-up mixing of the elevated PV in the concentric eyewalls leads to the formation of an AH. The time of the transition from concentric eyewalls to the AH is less than 24 hours, suggesting that the concentric eyewall replacement is an efficient route to AH formation. The results demonstrate potential capability of the WRF model to predict concentric eyewall cycles, the formation of AHs and associated intensity changes. **Citation:** Zhou, X., and B. Wang (2009), From concentric eyewall to annular hurricane: A numerical study with the cloud-resolved WRF model, *Geophys. Res. Lett.*, *36*, L03802, doi:10.1029/2008GL036854.

1. Introduction

[2] While the hurricane tracks can now be predicted with fidelity, the improvement of intensity forecast has been very limited over the past few decades. The primary reason for the slow improvement is associated with the difficulties in discerning and simulating the details of storm inner core. Recently, particular attentions have been focused on the formation of concentric eyewalls and annular hurricanes (AH) due to their distinctive features and close connections with hurricane intensity [Houze *et al.*, 2007; Knaff *et al.*, 2003, 2008].

[3] Concentric eyewalls usually refer to two or more eyewalls nearly concentric to the storm center. They are very common in the intense hurricanes. Over 50% of all tropical cyclones (TCs) attaining at least 60 m/s wind speeds undergo the concentric eyewall replacement cycle [Hawkins *et al.*, 2006]. In these hurricanes the asymmetric outer rainbands form their own convective ring (secondary eyewall) in coincidence with a local tangential wind maximum around the pre-existing eyewall [Willoughby *et al.*, 1982]. The secondary eyewall robs the inner eyewall of its needed moisture and angular momentum [Samsury and

Zipser, 1995] and creates hostile conditions to the inner eyewall [Barnes *et al.*, 1983; Rozoff *et al.*, 2008]. As a result the inner eyewall weakens and is eventually replaced by the outer eyewall. A weakening followed by a reintensification usually accompanies the eyewall replacement cycle. The large intensity fluctuation is a challenge for forecasters.

[4] Knaff *et al.* [2003] introduced a new category of tropical cyclones called annular hurricanes (AH) based on infrared satellite images and aircraft reconnaissance data. An AH, just as its name implies, is an annulus (large “circle”). It has a wide and nearly axially symmetric eyewall, a large circular eye, little or no rain bands outside the ring, and high intensity. The occurrence of AH is rare (about 4% of all hurricanes). Of particular interest is that AHs tend to persist, even when encountering the environmental conditions that can easily dissipate most other hurricanes. As a result, AHs pose an interesting challenge when forecasting hurricane intensity.

[5] Over the past years, there have been improvements in our ability to observe concentric eyewalls and AHs through in-situ means and by remote sensing [e.g., Houze *et al.*, 2007]. Observations shows that concentric eyewalls can lead to the formation of an AH [Kossin and Sitkowski, 2009]. For instance, the annular hurricane Daniel (2006) over the Eastern Pacific started out with a small eye (http://www.nrlmry.navy.mil/tc_pages/tc_home.html). It presents prominent annular structures after the concentric eyewall replacement [Knaff *et al.*, 2008]. However, the detailed transformation processes have not been understood.

[6] Some efforts have been made in the numerical modeling of the formation of concentric eyewall or AHs, but not the potential linkage between these two specific eyewall features. For example, the recent high-resolution numerical simulations in concentric eyewalls by Houze *et al.* [2007], Terwey and Montgomery [2008] are very encouraging, although prediction of the timing and intensity modulation due to eyewall replacement remains problematic. Wang [2008] studied the formation of an AH with a full-physical model in a resting environment. The interaction between the inner spiral rainband and the eyewall is attributed to formation of an annular hurricane, but the transition took 96 hr, which is much longer than observed (24 hr). The fast transition to AHs as observed remains elusive.

[7] The Weather Research and Forecasting (WRF) model has been extensively used in both the hurricane operational forecast and research. However the concentric eyewall replacement cycle has not been simulated by this model. This paper reports that the WRF model is capable of simulating the succession of concentric eyewall replacement. More interestingly, we found the concentric eyewall replacement lead to the formation of an AH, and this

¹Department of Meteorology, School of Ocean and Earth Science and Technology, University of Hawaii at Mānoa, Honolulu, Hawaii, USA.

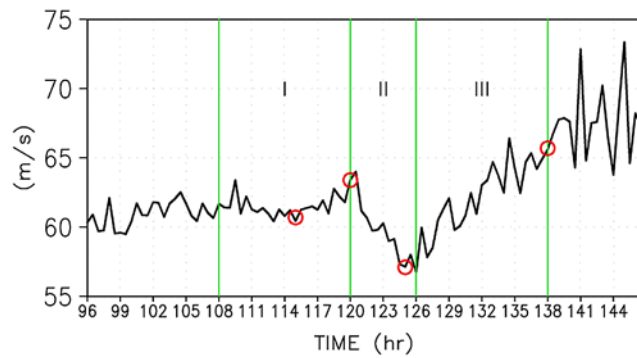


Figure 1. Time series of the maximum wind speed at the surface (m/s) simulated by the WRF model. Green thin lines denote three phases in the eyewall replacement cycle. Open circles correspond to the time in Figures 3 and 4.

formation process takes less than 24 hours, which is similar to the observed rapid formation [Knaff *et al.*, 2003].

2. Experimental Design

[8] The WRF model used in this study is quadrupely nested with two-way interaction. The horizontal resolutions are 54, 18, 6, and 2 km respectively with 28 levels in the vertical. The Kain-Fritsch convective scheme was applied in the two outermost meshes, and only explicit cloud scheme was used in the two inner meshes.

[9] The model is initialized with an axisymmetric cyclonic vortex on an f plane located at 18°N in a quiescent environment with a constant sea surface temperature of 29°C . The initial cyclonic vortex has a maximum surface wind speed of 15 m/s at a radius of 150 km and the wind speed decreases with height. The mass and thermodynamic fields were obtained by solving the nonlinear balance equation for the given tangential wind field. All the param-

eter settings for the initial vortex are identical to that described by *Ge et al.* [2008].

3. Results

[10] The vortex spins up rapidly in the first 48 hr and then reaches a relatively steady state with a maximum wind speed of 60 m/s (not shown). The storm begins weakening at 120 hr but reintensifies from 126 hr to 138 hr (Figure 1). The maximum wind reaches about 65 m/s with a significant fluctuation. As we shall see latter, the weakening and reintensification of the storm are associated with the formation of a secondary eyewall, the eyewall replacement and the eventual formation of an AH.

[11] The simulated life cycle of the concentric eyewalls consists of three distinctive phases (Figure 2), which corresponds well to the intensity changes shown in Figure 1. In phase I (108–120 hr), the storm intensity remains almost constant. New convection outside the eyewall emerges at about 140 km away from the hurricane center as evidenced by the axially symmetric upward motion. It moves inward and amplifies rapidly at the end of the first stage in the vicinity of the 70 km at radius (Figure 2a). In Phase II (120–126 hr) the intensity drops from 65 m/s to 57 m/s (Figure 1). The storm exhibits two deep convective updrafts. With time the inner convective updraft becomes thinner and weaker and the outer one becomes broader and stronger. On the other hand, the outer periphery of the 700 hPa wind speed exceeding 60 m/s expands rapidly from 65 km to 90 km. Figure 2b shows that a secondary tangential wind maximum corresponding to the secondary eyewall develops outside the inner eyewall. It becomes nearly as strong as the old eyewall at the end of the replacement. Furthermore the radial gradient of the tangential wind reduces significantly. In phase III (126–138 hr), the old eyewall vanishes and the new eyewall dominates. The radius of the maximum wind (RMW) changes from 40 km to 70 km as a result of the eyewall replacement. With

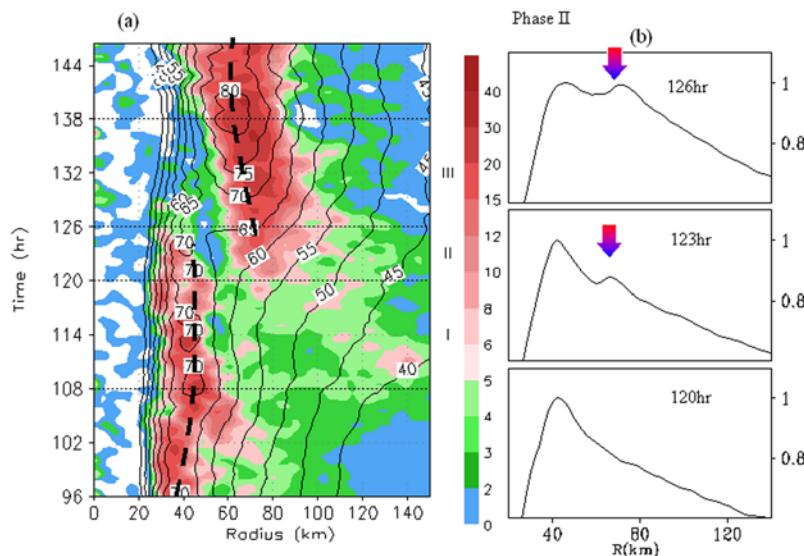


Figure 2. (a) Radius-time Hovmöller diagrams of the azimuthal mean vertical velocity in 500 hPa (shading, cm/s) and tangential velocity in 700 hPa (contour, m/s). (b) Tangential wind profile in 700 hPa during the phase II normalized by the maximum wind.

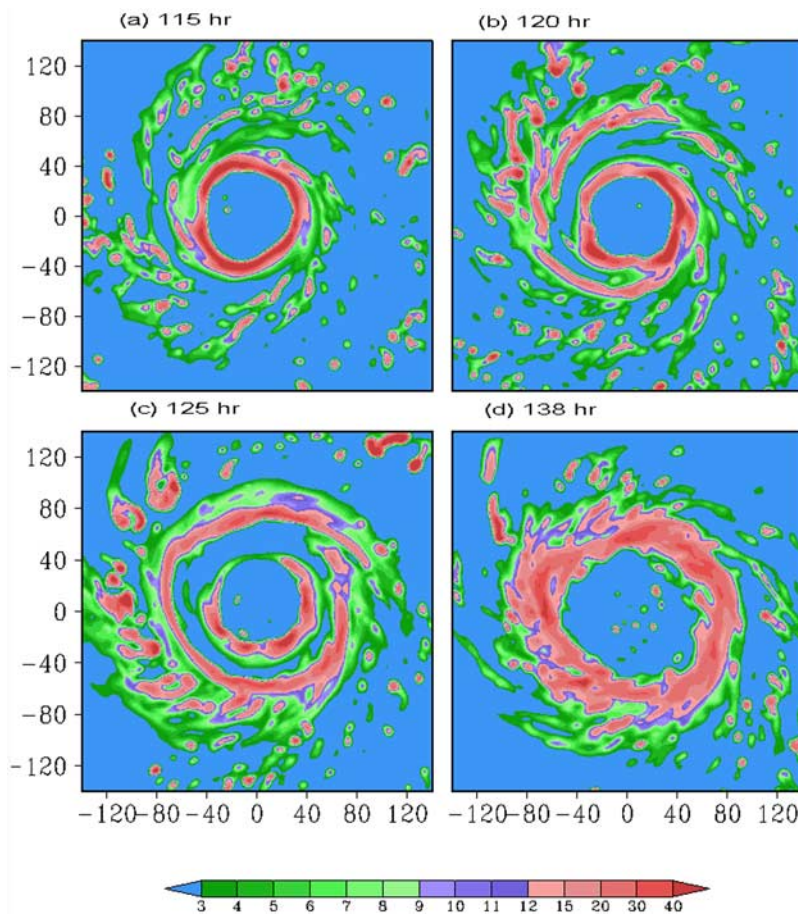


Figure 3. Simulated rainwater distributions (0.1 g/kg) in 550 hPa at (a) 115 hr, (b) 120 hr, (c) 125 hr and (d) 138 hr.

the contraction and strengthening of the new eyewall, the storm increases the maximum winds from 57 m/s at 126 hr to 67 m/s at 138 hr (Figure 1). Similar to the most observed concentric eyewalls [Willoughby *et al.*, 1982], the new eyewall contracts slightly but does not fully reduce to the size of the original eyewall.

[12] A sequence of storm structures during the different stages of the concentric eyewall cycle is shown in Figure 3. The original eyewall is a thin annulus of high rainwater concentration (Figure 3a). Outside the eyewall are active convective cells organized into several loosely defined spiral rainbands. Figure 3b shows that a large spiral rainband, usually referred to as a principal rainband, spirals into and connects to the eyewall. Thereafter the spiral arrangement of convection becomes a convective ring (Figure 3c). Note that the storm starts to weaken (120 hr) prior to the formation of the secondary eyewall from the principal rainband. It indicates that the spiral rainband with vigorous convection acts as a partial barrier creating hostile conditions to the inner eyewall [Barnes *et al.*, 1983]. It plays a similar role as the secondary eyewall in the destruction of the inner eyewall. Figure 3d illustrated that the storm contains all typical characteristics of an AH after the eyewall replacement: quasi-axisymmetric structures, a large-size eye, a thick eyewall, fewer major spiral rainbands, as well as high intensity.

[13] In an effort to better view the eyewall evolution, the radial-vertical cross section of the azimuthally mean tan-

gential wind and vertical velocity is illustrated in Figure 4. Apparently the outer eyewall presents a larger outward vertical tilt than the inner one's. Similar characteristic is documented in Hurricane Rita (2005) during Hurricane Rainband and Intensity Change Experiment (RAINEX). The dual-Doppler storm-relative winds derived from Electra Doppler radar (ELDORA) show the deep updraft of the secondary eyewall in Hurricane Rita (2005) has much larger outward tilt in the vertical [Houze *et al.*, 2007, Figure 2d]. In addition, Figure 4 illustrates that the appearance of the secondary convective maximum precedes that of the secondary wind maximum. A closer look will show that the local outer wind maximum primarily present in the lower to middle troposphere at the radius outside of the secondary convection maximum. Two separated wind peaks are absent near the surface despite of the small radial tangential wind gradient.

[14] Convections in the secondary eyewall typically contain a well-defined tangential wind maximum, analogous to the peak winds in the inner eyewall. The two tangential wind maxima are associated with relatively enhanced vorticity so that the radial gradient of vorticity changes the sign at least twice from the central vortex to the outer eyewall. When the moat between the inner and outer ring is sufficiently narrow, the barotropic instability may occur (referred as type II instability by Kossin *et al.* [2000]). Since the outer eyewall has larger outward tilt with height, the moat between the two eyewall is relatively narrow near the

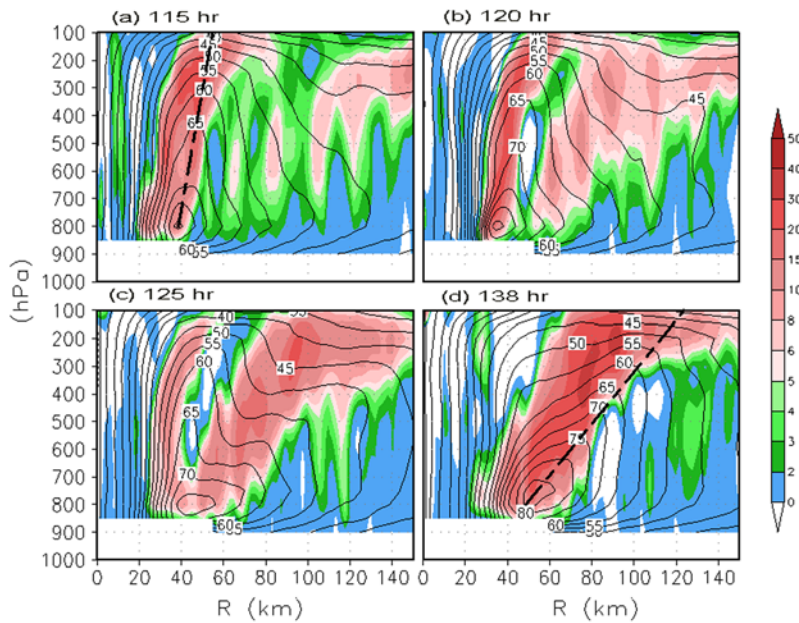


Figure 4. Simulated radius-vertical distributions of azimuthal mean vertical velocity (shading, cm/s) and tangential wind (contour, m/s) at (a) 115 hr, (b) 120 hr, (c) 125 hr and (d) 138 hr.

surface. The nonlinear mixing between concentric eyewalls would result into the absence of two separated wind maxima near the surface. By examining the radius-vertical distributions of azimuthally averaged potential vorticity (PV), it is found that the PV mixing between concentric eyewalls is evidence (Figure 5). The enhanced PV in the inner and outer eyewall mixes gradually from the lower to the upper level during and after the eyewall replacement. The bottom-up mixing eventually forms a wide enhanced PV region, thus the weak radial shear of the tangential wind from the lower to upper troposphere. Figure 2b shows that the tangential wind profile in 700hPa becomes much flatter after the

eyewall replacement. Corresponding to the low differential rotational speed, the thickness of the new eyewall is almost double the original one (Figure 4a). Apparently, the sufficient PV mixing between the concentric eyewalls contributes to the formation of the wide annular eyewall.

4. Summary and Discussion

[15] Recent observations show that annular hurricanes may form after an eyewall replacement cycle but radar and satellite images provide very limited information and little is known about how they form and evolve. The present

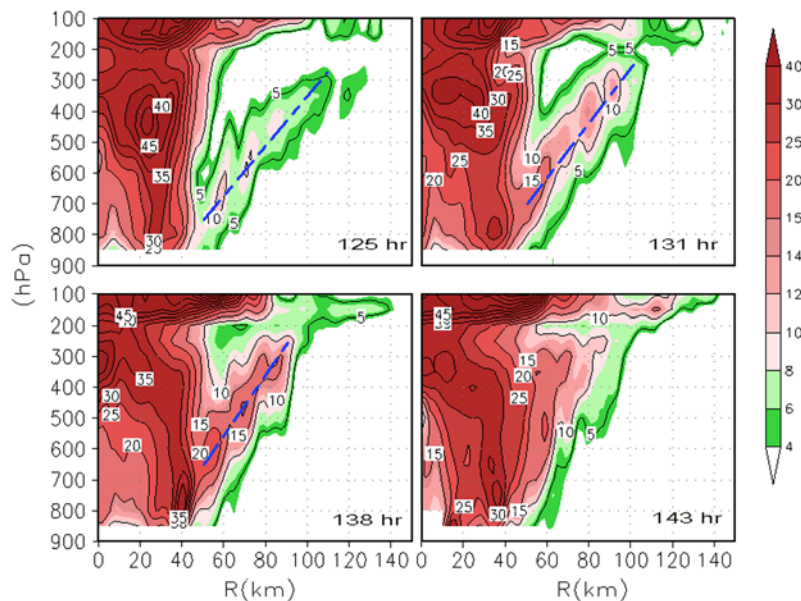


Figure 5. Simulated radius-vertical distributions of potential vorticity (0.1 PVU) during and after the eyewall replacement.

modelling study shows that this type of inner-core processes can be simulated with the high-resolution (2 km) WRF model. In a resting environment on a constant f plane, the storm undergoes the formation of the concentric eyewall, the eyewall replacement, and ends up with an annular hurricane. The simulated replacement process is very similar to the conventional concentric eyewall cycle previously studied [Willoughby *et al.*, 1982]. The storm evolves into an AH within 24 hours after the eyewall replacement. This fast formation is consistent with the observation [Knaff *et al.*, 2003]. The results suggest that the concentric eyewall is an efficient route to form an AH. Evidence is shown that the AH formation is related to the significant mixing of the enhanced PV in the concentric. Several issues related to the eyewall processes simulated in the model are further discussed as follows.

[16] The concentric eyewall replacement often coincides with a weakening of hurricane intensity, but by no means necessarily. The associated intensity change and the time of eyewall replacement vary with cases [Willoughby *et al.*, 1982]. For example, the appearance of the concentric eyewall in Hurricane Anita (1977) only marks the end of a deepening phase, but an abrupt decrease in maximum wind speed as large as 46 m/s is detected in Typhoon Sarah (1956). By summarizing several cases of concentric eyewall, Willoughby [1995] addressed that the timing required for a cycling of weakening and reintensification can range from a few hours to more than a day. In our case the eyewall replacement process is quite fast (about 6 hr) and there is no dramatic intensity fluctuation (8–10 m/s). On the other hand, a vigorous secondary eyewall develops rapidly and becomes quite intense at the end of the replacement. The abrupt development of the outer eyewall likely leads to a quick replacement and a little intensity change. To provide accurate intensity forecasts, attentions should be paid not only on whether the secondary eyewalls form or not, but also the strength and radial locations of the secondary eyewall.

[17] Theoretical understanding for the formation of AH is still in infancy. Knaff *et al.*, [2003] investigated the environmental conditions favorable for AHs. Wang's [2008] numerical study shows that the inward contraction of the inner spiral rainband forms an AH, but the transition from the non-AH to the annular one was slow and gradual (96 hr). Our study suggests that secondary eyewall replacement may be another route for the rapid formation of an AH. However, not all hurricanes with concentric eyewalls turn into an AH. The evidence in this study shows that the PV mixing between concentric eyewalls due to barotropic instability likely lead to the formation of a AH. Thus an important consideration probably is how close the secondary eyewall is likely to initiate to the inner eyewall. Further

observational investigations are required to examine the dependence of the formation of a AH on the radial location of the secondary eyewall. Admittedly, the large-scale environment could play a role in the formation of secondary eyewall as well as AH, but they are not considered in the present study.

[18] **Acknowledgments.** The authors thank Xuyang Ge for providing the WRF initialization code of tropical cyclone and stimulating discussions. Gary Barnes and Liguang Wu made valuable comments on an earlier version of the manuscript. U.S. Office of Naval Research under grant N00014-021-0532 supports this research. This is publication 7610 of the School of Ocean and Earth Science and Technology and the International Pacific Research Center publication 575.

References

- Barnes, G. M., E. J. Zipser, D. P. Jorgensen, and F. D. Marks Jr. (1983), Mesoscale and convective structure of a hurricane rainband, *J. Atmos. Sci.*, **40**, 2125–2137.
- Ge, X., T. Li, Y. Wang, and M. Peng (2008), Tropical cyclone energy dispersion in a three-dimensional primitive equation model: Upper tropospheric influence, *J. Atmos. Sci.*, **65**, 2272–2289.
- Hawkins, J. D., M. Helveston, T. F. Lee, F. J. Turk, K. Richardson, C. Sampson, J. Kent, and R. Wade (2006), Tropical cyclone multiple eyewall configurations, paper presented at 27th Conference on Hurricanes and Tropical Meteorology, Am. Meteorol. Soc., Monterey, Calif.
- Houze, R. A., S. S. Chen, B. F. Smull, W.-C. Lee, and M. M. Bell (2007), Hurricane intensity and eyewall replacement, *Science*, **315**, 1235–1239.
- Knaff, J. A., J. P. Kossin, and M. DeMaria (2003), Annular hurricanes, *Weather Forecast*, **18**, 204–223.
- Knaff, J. A., T. A. Cram, A. B. Schumacher, J. P. Kossin, and M. DeMaria (2008), Objective identification of annular hurricanes, *Weather Forecast*, **23**, 17–88.
- Kossin, J. P., and M. Sitkowski (2009), An objective model for identifying secondary eyewall formation in hurricanes, *Mon. Weather Rev.*, in press.
- Kossin, J. P., W. H. Schubert, and M. T. Montgomery (2000), Unstable interactions between a hurricane's primary eyewall and a secondary ring of enhanced vorticity, *J. Atmos. Sci.*, **57**, 3893–3917.
- Rozoff, C. M., W. H. Schubert, and J. P. Kossin (2008), Some dynamical aspects of tropical cyclone concentric eyewalls, *Q. J. R. Meteorol. Soc.*, **134**, 583–593.
- Samsury, C. E., and E. J. Zipser (1995), Secondary wind maxima in hurricanes: Airflow and relationship to rainbands, *Mon. Weather Rev.*, **123**, 3502–3517.
- Terwey, W. D., and M. T. Montgomery (2008), Secondary eyewall formation in two idealized, full-physics modeled hurricanes, *J. Geophys. Res.*, **113**, D12112, doi:10.1029/2007JD008897.
- Willoughby, H. E. (1995), Mature structure and evolution tropical cyclone structure and structure change, in *Global Perspectives on Tropical Cyclones*, Rep. TCP-38, edited by R. L. Elsberry, pp. 21–62, World Meteorol. Organ., Geneva, Switzerland.
- Willoughby, H. E., J. A. Clos, and M. G. Shoreibah (1982), Concentric eyewalls, secondary wind maxima, and the evolution of the hurricane vortex, *J. Atmos. Sci.*, **39**, 395–411.
- Wang, Y. (2008), Structure and formation of an annular hurricane simulated in a fully compressible, nonhydrostatic model—TCM4, *J. Atmos. Sci.*, **65**, 1505–1527.

B. Wang and X. Zhou, Department of Meteorology, School of Ocean and Earth Science and Technology, University of Hawaii at Mānoa, 2525 Correa Rd., HIG 351A, Honolulu, HI 96822, USA. (xiaqiong@hawaii.edu)